fornica (*18*). Electrophysiology was performed as previously described (*18*), with the exception that sensory cells were stimulated extracellularly.
20. T. Sollner *et al.*, *Nature* **362**, 318 (1993).
21. J. M. Hunt *et al.*, *Neuron* **12**, 1269 (1994).
22. L. Edelmann, P. I. Hanson, E. R. Chapman, R. Jahn, *EMBO J.* **14**, 224 (1995).
23. T. Sollner, M. K. Bennett, S. W. Whiteheart, R. H. Scheller, J. E. Rothman, *Cell* **75**, 409 (1993).
24. J. V. Frangioni and B. G. Neel, *Anal. Biochem.* **210**, 179 (1993).
25. D. Bartsch, in preparation.
26. G. J. Chin, E. Shapiro, S. S. Vogel, J. H. Schwartz, *J. Neurosci.* **9**, 38 (1989).
27. Five-day-old primary cocultures of *Aplysia* sensory and motor neurons were washed in phosphate-buffered saline (PBS) containing 30% (w/v) sucrose and then fixed with 4% (w/v) paraformaldehyde in the same solution. Cell membranes were permeabilized with 0.1% Triton X-100 in PBS and the fixative was quenched with 50 mM NH_4Cl. After blocking nonspecific interactions with 10% (v/v) goat serum in PBS containing 30% sucrose, the cells were incubated with either preimmune serum or VAP-33–specific antiserum prepared against the full-length polypeptide expressed in bacteria as a polyhistidine-tagged fusion protein by using the vector pET-30a (Novagen) (dilution of 1:400 in blocking solution). Immunoreactivity was visualized with Cy3-conjugated goat antibodies to rabbit immunoglobulin (Jackson Immunoresearch) at 1:200 in blocking solution.
28. We would like to thank M. Ghirardi for technical advice and helpful discussions and H. Zhu for technical assistance. C. Lam and R. Baston helped with figures, and H. Ayers and A. Krawetz typed the manuscript. Supported by the Howard Hughes Medical Institute and by the National Institute of Mental Health (R37 MH45923-06).

28 March 1995; accepted 5 July 1995

Requirement of MIP-1α for an Inflammatory Response to Viral Infection

Donald N. Cook,* Melinda A. Beck, Thomas M. Coffman, Suzanne L. Kirby, John F. Sheridan, Ian B. Pragnell, Oliver Smithies

Macrophage inflammatory protein–1α (MIP-1α) is a chemokine that has pro-inflammatory and stem cell inhibitory activities in vitro. Its biologic role in vivo was examined in mice in which the gene encoding MIP-1α had been disrupted. Homozygous MIP-1α mutant (−/−) mice were resistant to Coxsackievirus-induced myocarditis seen in infected wild-type (+/+) mice. Influenza virus–infected −/− mice had reduced pneumonitis and delayed clearance of the virus compared with infected +/+ mice. The −/− mice had no overt hematopoietic abnormalities. These results demonstrate that MIP-1α is an important mediator of virus-induced inflammation in vivo.

The recruitment of leukocytes to sites of infection is crucial to the inflammatory clearance of pathogens. Various molecules may control leukocyte trafficking in vivo, including the chemokines, a family of low molecular weight proteins that induce leukocyte chemotaxis in vitro (*1*). MIP-1α is a member of the β chemokine subfamily, which also includes MIP-1β and RANTES. MIP-1α induces chemotaxis of monocytes, $CD8^+$ T cells (*2*), $CD4^+$ T cells, and B cells in vitro (*3*). However, the importance of MIP-1α in vivo has been unclear, because many of its activities are shared by other β chemokines, including an ability to bind to the same receptor (*4*). To determine its function in vivo, we used homologous recombination in mouse strain 129–derived embryonic stem (ES) cells to generate a deletion in the MIP-1α gene. The deletion included 300 nucleotides (nt) of DNA upstream of the mRNA start site, as well as the first exon and half of the second exon of the MIP-1α gene (Fig. 1). Injection of these cells into C57BL/6J blastocysts produced nine chimeras, five of which transmitted the mutant MIP-1α allele to the offspring. Matings between F_1 heterozygotes (+/−) yielded offspring of the MIP-1α genotypes +/+, +/−, and −/− in Mendelian proportions. The −/− mice had no gross abnormalities in development or in the histology of any major organ.

To examine MIP-1α expression in −/− mice, we isolated bone marrow macrophages, stimulated them with L929 cell–conditioned media (*5*), and prepared RNA. Northern (RNA) blot analysis with a MIP-1α complementary DNA (cDNA) probe revealed abundant MIP-1α mRNA (780 nt) in +/+ mice, less mRNA in +/− mice, and essentially no mRNA in the −/− mice (Fig. 1E). Because the deletion includes almost half of the MIP-1α coding region, any mRNAs transcribed from the mutant MIP-1α locus are unlikely to encode a functional protein.

MIP-1α inhibits the proliferation of early hematopoietic progenitor cells in vitro (*6*). Therefore, we compared the peripheral blood and bone marrow of +/+ mice to that of −/− mice to determine whether the mutation had affected hematopoiesis. No significant differences between the two genotypes were observed in peripheral blood (hematocrits, total white blood cell counts, and differential counts) or in bone marrow [total nucleated cells per femur and early hematopoietic progenitor cell number (*7*)] (two-tailed *t* test). Analysis of cell populations in lymph nodes and spleens revealed that both T and B cell numbers in the −/− mice were indistinguishable from those of +/+ mice. Thus, the −/− mice lack any overt hematopoietic abnormalities.

In light of evidence for a role of MIP-1α in autoimmune disease (*8*), we tested the response of the −/− mice to Coxsackievirus B3 (CVB3). CVB3 infection of humans is a major cause of myocarditis in young adults, and in neonates it is frequently lethal. CVB3 also induces myocarditis in various strains of mice, and the pathophysiology closely resembles that of humans; macrophages and neutrophils accumulate in the heart around day 5 postinfection (p.i.) and are gradually replaced by a T cell infiltrate by day 10 p.i. Substantial evidence suggests that the cardiac lesions result from an autoimmune mechanism mediated primarily by cytotoxic T lymphocytes, although direct viral-mediated cytopathology may also occur (*9*).

To determine the role of MIP-1α in CVB3-induced myocarditis, we killed mice at various times after infection and analyzed histologic sections of heart by light microscopy (*10*). Cardiac lesions were first observed in +/+ mice at day 6 p.i.; at days 10, 15, and 21 p.i., the majority of +/+ mice had moderate to severe myocarditis (Fig. 2). The lesions were characterized by a mononuclear cell infiltrate and evidence of cytolysis. In contrast, none of the −/− mice had myocarditis or evidence of cytolysis at any time.

To test whether some unidentified, natural, strain-specific differences between 129 and C57BL/6J mice at or near the β chemokine locus may account for the observed difference in inflammation between the two groups, we interbred +/+ mice having 129-derived DNA at the β chemokine locus (129+/129+) and infected them with CVB3 (*11*). Three of five infected 129+/129+ mice developed myocarditis, whereas none of an additional five −/− mice had inflammation. This result demonstrates

D. N. Cook and O. Smithies, Department of Pathology, University of North Carolina, Chapel Hill, NC 27599–7525, USA.
M. A. Beck, Department of Pediatrics, University of North Carolina, Chapel Hill, NC 27599–8180, USA.
T. M. Coffman, Department of Internal Medicine, Durham Veterans Affairs Medical Center, Durham, NC 27710, USA.
S. L. Kirby, Department of Medicine, University of North Carolina, Chapel Hill, NC 27599–7035, USA.
J. F. Sheridan, Departments of Oral Biology and Medical Microbiology and Immunology, Ohio State Health Sciences Center, Columbus, OH 43210–1239, USA.
I. B. Pragnell, CRC Beatson Laboratories, Bearsden, Glasgow, G61 1BD, UK.
*To whom correspondence should be addressed.

that any natural, strain-specific differences between 129 and C57BL/6J mice are not the cause of the difference in myocarditis between −/− and +/+ mice. The difference must therefore be a direct consequence of the MIP-1α mutation.

We tested splenocytes for reactivity in vitro (*10*) to determine whether the absence of myocarditis in CVB3-infected (−/−) mice was related to a general defect in T cell function. Incorporation of [^{3}H]thymidine in splenocytes from MIP-1α −/− mice was indistinguishable from that of +/+ controls in response to either conconavalin A [−/−, $6.7 \pm 2.2 \times 10^4$ cpm; +/+, $7.8 \pm 1 \times 10^4$ cpm] or inactivated CVB3 virus [−/−, $28 \pm 3 \times 10^3$ cpm; +/+, $29 \pm 3 \times 10^3$ cpm]. The CVB3-neutralizing antibody titer [determined by testing serum dilutions for virus neutralizing activity (*10*)] in the −/− mice (1/311 ± 83) did not differ from +/+ mice (1/407 ± 118). These data indicate that antigen processing, T cell activation, and B cell differentiation are normal in the −/− animals, and the data suggest that the absence of myocarditis in the MIP-1α −/− mice is likely because of an inability to recruit or retain mononuclear cells in the infected heart. These results may have implications for therapeutic intervention in myocarditis for which no effective treatment is currently available.

We determined how the absence of inflammatory cell infiltrate in the −/− mice affected viral titers at day 10 p.i. The geometric mean of viral titers in −/− mice [3.43 ± 0.8 tissue culture infectious dose ($TCID_{50}$) per gram of tissue] (*10*) was indistinguishable from that of +/+ controls (3.01 ± 0.9 $TCID_{50}$). This result is consistent with the observation that mice depleted of T cells have reduced myocarditis but do not have increased viral titers (*12*). Together, these data suggest that CVB3-medi-

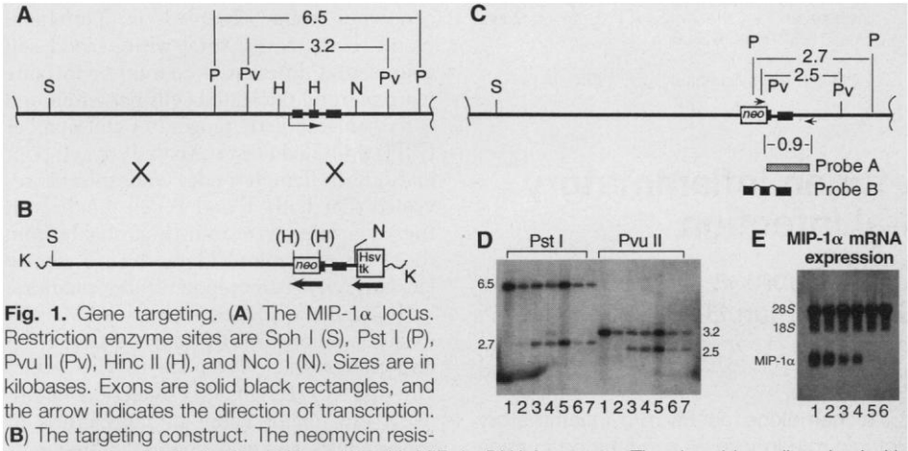

Fig. 1. Gene targeting. (**A**) The MIP-1α locus. Restriction enzyme sites are Sph I (S), Pst I (P), Pvu II (Pv), Hinc II (H), and Nco I (N). Sizes are in kilobases. Exons are solid black rectangles, and the arrow indicates the direction of transcription. (**B**) The targeting construct. The neomycin resistance gene (*neo*) is flanked by 9-kb and 0.9-kb MIP-1α DNA fragments. The plasmid was linearized with Kpn I (K) before it was electroporated into the ES cell line BK4 [a subclone of E14TG2A (*18*)]. The X's denote homologous recombination, and Hsv tk is the herpes simplex virus thymidine kinase gene. (**C**) Structure of the targeted locus. The sizes of the expected fragments are shown in kilobases. Arrowheads represent the *neo* primer (5′-TAAAGCGCATGCTCCAGACT-3′) and the MIP-1α primer (5′-GAAGTGGAGAAGTCTACTCCA-3′) used for polymerase chain reaction amplification (*19*). Probe A was used for Southern (DNA) blots and probe B for Northern (RNA) blots. (**D**) Southern blots of DNA from BK4 cells (lane 1) and from six independently targeted cell lines (lanes 2 through 7) confirm the targeting event. The sizes of the DNA fragments are indicated in kilobases. (**E**) Analysis of MIP-1α mRNA expression. RNA was isolated from macrophage cultures of +/+ (lanes 1 and 2), +/− (lanes 3 and 4), and −/− (lanes 5 and 6) mice as in (*5*). RNA blots were hybridized with MIP-1α cDNA, then rehybridized with oligonucleotides corresponding to 18*S* and 28*S* ribosomal RNAs to verify equal loading.

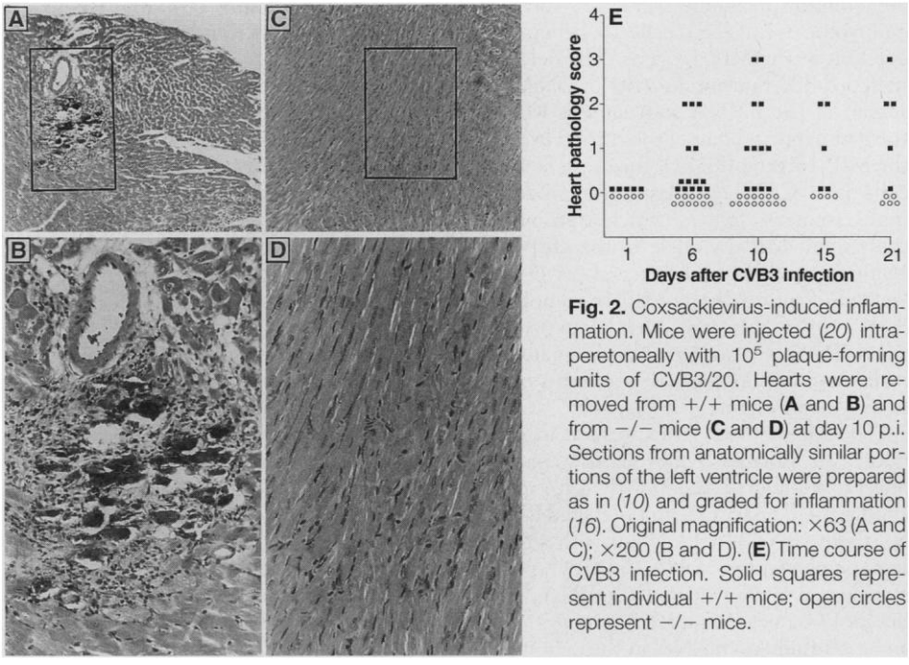

Fig. 2. Coxsackievirus-induced inflammation. Mice were injected (*20*) intraperetoneally with 10^5 plaque-forming units of CVB3/20. Hearts were removed from +/+ mice (**A** and **B**) and from −/− mice (**C** and **D**) at day 10 p.i. Sections from anatomically similar portions of the left ventricle were prepared as in (*10*) and graded for inflammation (*16*). Original magnification: ×63 (A and C); ×200 (B and D). (**E**) Time course of CVB3 infection. Solid squares represent individual +/+ mice; open circles represent −/− mice.

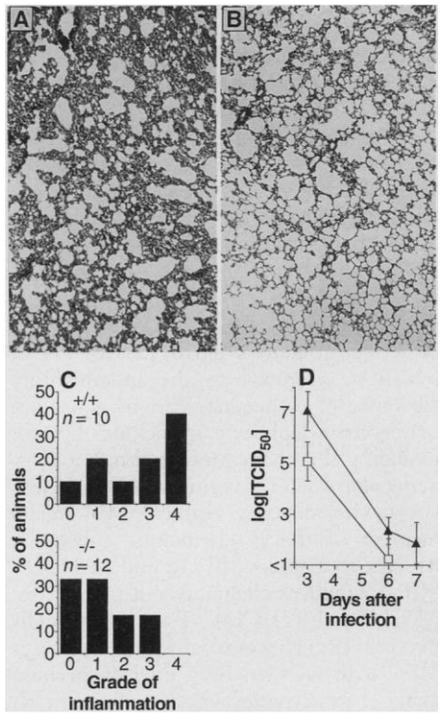

Fig. 3. Influenza virus–induced inflammation. Histologic sections of lung from influenza A/Puerto Rico/8/34 virus–infected mice at day 7 p.i. Lungs were formalin-fixed, paraffin-imbedded, and cut sections were stained with hematoxylin and eosin. Inflammation was graded on a scale of 0+ to 4+ (*16*). A representative section of grade 3 is shown from a +/+ mouse (**A**), and of grade 1 from a −/− mouse (**B**). (**C**) Analysis of inflammation. The percentage of animals assigned to each grade is shown for both genotypes. (**D**) Clearance of influenza virus. Viral titers in lung homogenates were determined for +/+ mice (open squares) and −/− mice (solid triangles) by $TCID_{50}$ on canine kidney cells. Bars represent standard error.

ated cardiac damage in normal mice is not the result of viral-mediated cytolysis, but rather is from the actions of recruited inflammatory cells. The data are also consistent with, but do not prove, a requirement of MIP-1α in an autoimmune-mediated model of CVB3-induced myocarditis. In this regard, it is noteworthy that antibodies to MIP-1α reduce the severity of experimental autoimmune encephalomyelitis (8), and that the murine MIP-1α gene maps to a region of chromosome 11 that includes the Idd4 insulin-dependent diabetes locus (13).

We infected −/− mice with influenza virus to examine the inflammatory response to a pathogen of different tissue tropism. This model was chosen because pulmonary alveolar macrophages are a rich source of MIP-1α (14), suggesting that it may be involved in pulmonary inflammation. Influenza-infected mice were killed at day 6 or 7 p.i., when pathology is maximum (15). The lungs of most of the +/+ animals were inflamed and edematous; those of the −/− mice were less severely affected. Histologic sections of lung were graded for inflammation between 0+ and 4+ (16), on the basis of the extent of mononuclear cell infiltration and tissue damage (Fig. 3). The +/+ mice had significantly more inflammation than −/− mice ($P = 0.012$ by the Wilcoxon rank order test). These data demonstrate that MIP-1α contributes to influenza virus–induced pneumonitis.

Influenza virus is generally cleared from the lungs of immunocompetent mice by 6 to 10 days p.i. by a T cell–dependent mechanism (17). To determine whether MIP-1α affects influenza virus clearance, we measured viral titers at various times after infection and calculated the geometric mean for each genotype (Fig. 3D). Viral titers were higher in −/− animals compared with +/+ controls at day 3 p.i. ($P = 0.14$ by the two-tailed t test) and significantly so at days 6 and 7 p.i. ($P = 0.02$). Part of this difference may be accounted for by the increased weight of the +/+ lungs, but this weight difference was at most twofold, whereas the difference in viral titers was 100- to 1000-fold. By day 21 p.i., no virus was detected in either group of mice. This delay in T cell–dependent viral clearance in the −/− mice suggests that MIP-1α may be required for efficient recruitment of immunocompetent T cells to sites of viral infection, which is consistent with the ability of the chemokine to induce chemotaxis of T cells in vitro (2, 3).

Our experiments provide genetic evidence for the requirement of a β chemokine in inflammation and demonstrate that other chemokines do not functionally substitute for MIP-1α. The relative importance of MIP-1α in an inflammatory response may depend on the pathogen or tissue involved, possibly because of the expression of other molecules with compensatory activity. Nevertheless, the role of MIP-1α in diseases as different as myocarditis and pneumonitis suggests that this chemokine may also mediate inflammation in response to a variety of other stimuli.

REFERENCES AND NOTES

1. D. J. Kelvin, *et al.*, *J. Leukoc. Biol.* **54**, 604 (1993).
2. D. D. Taub, K. Conlon, A. R. Lloyd, J. J. Oppenheim, D. J. Kelvin, *Science* **260**, 355 (1993).
3. T. J. Schall, K. Bacon, R. D. Camp, J. W. Kaspari, D. V. Goeddel, *J. Exp. Med.* **177**, 1821 (1993).
4. K. Neote, D. DiGregorio, J. Y. Mak, R. Horuk, T. Schall, *Cell* **72**, 415 (1993).
5. J. Maltman, I. B. Pragnell, G. J. Graham, *J. Exp. Med.* **178**, 925 (1994).
6. G. J. Graham *et al.*, *Nature* **344**, 442 (1990).
7. I. B. Pragnell *et al.*, *Blood* **72**, 196 (1988).
8. W. Karpus *et al.*, *J. Immunol.* **8** (abstr.), 1148 (1994).
9. J. F. Woodruff, *Am. J. Pathol.* **101**, 425 (1980).
10. M. Beck *et al.*, *J. Nutr.* **124**, 345 (1994).
11. We interbred +/+ F_1 mice that have 129- and C57BL/6J-derived β chemokine loci and identified F_2 offspring homozygous for the 129-derived β chemokine locus by a Pst I restriction fragment length polymorphism.
12. J. F. Woodruff and J. J. Woodruff, *J. Immunol.* **113**, 1726 (1974).
13. B. M. Gill, A. Jamarillo, L. Ma, K. B. Laupland, T. Delovitch, *Diabetes* **44**, 614 (1995).
14. K. E. Driscoll, D. G. Hassenbein, J. Carter, *Am. J. Respir. Cell. Mol. Biol.* **8**, 311 (1993).
15. G. Hermann, F. M. Beck, J. F. Sheridan, *J. Neuroimmunol.* **56**, 179 (1995).
16. Grading of inflammation in all experiments was done without prior knowledge of the mouse genotypes.
17. P. C. Doherty, W. Allen, M. Eichelberger, *Annu. Rev. Immunol.* **10**, 123 (1992).
18. M. Hooper *et al.*, *Nature* **326**, 292 (1987).
19. H. S. Kim and O. Smithies, *Nucleic Acids Res.* **18**, 8887 (1988).
20. Animal experiments were conducted in accordance with institutional guidelines for the University of North Carolina at Chapel Hill.

21. We thank Q. Shi, K. Kluckman, J. Hagaman, T. Bone-Turrentine, and R. Reilly for technical assistance. Supported by grants GM20069 and HL37001 (O.S.) and R29HL46195 (M.A.B.) and the Cooley's Anemia Foundation (D.N.C.).

24 April 1995; accepted 21 July 1995

A Mechanism for the Specific Immunogenicity of Heat Shock Protein–Chaperoned Peptides

Ryuichiro Suto and Pramod K. Srivastava*

Endogenously synthesized antigenic determinants are generally presented on major histocompatibility complex (MHC) class I molecules, whereas exogenous determinants are presented by MHC class II molecules. Here, it is shown that exogenous antigens chaperoned by a heat shock protein can be channeled into the endogenous pathway, presented by MHC class I molecules, and recognized by $CD8^+$ T lymphocytes. This pathway is functional only in a subset of macrophages among the cell types tested. These observations provide a basis for the tumor-specific and virus-specific immunogenicity of cognate heat shock protein preparations and offer a mechanism for the classical phenomenon of cross-priming.

Heat shock proteins (HSPs) isolated from cancer cells or virus-infected cells elicit protective immunity or cytotoxic T lymphocytes (CTLs) to the cognate tumor or viral antigen (1–3). In contrast, HSPs isolated from normal tissues do not elicit such immunity (2, 3). Because the HSP genes do not show tumor-associated DNA polymorphism, it has been suggested that HSPs derived from cancers or virus-infected cells are not immunogenic per se but rather chaperone tumor- or virus-specific antigenic peptides generated during antigen processing, and that it is the peptides and not the HSPs that are immunogenic (4). This suggestion was upheld by the sequencing of a number of HSP-associated peptides (5) and by the observation that HSPs stripped of associated peptides lose their immunogenicity (3).

Department of Biological Sciences, Fordham University, Bronx, NY 10458, USA.

*To whom correspondence should be addressed.

One of the unresolved questions in this area has been the mechanism whereby HSP-peptide complexes elicit specific immunity. Immunogenicity of HSP preparations is exquisitely dependent on the presence of functional phagocytic cells in the host; the depletion of such cells rendered the host incapable of being immunized by HSP preparations (6). This observation led to the suggestion that HSPs are taken up by the macrophage and are re-presented by the MHC class I molecules of the macrophage, which finally stimulate the appropriate T cells (7). Thus, a mechanism of indirect presentation of HSP-chaperoned peptides was invoked. The observations reported here support this mechanism.

We have investigated whether HSP-chaperoned peptides could be re-presented by phagocytic cells in a vesicular stomatitis virus (VSV) model. The HSP gp96 was isolated to apparent homogeneity (8) from EL4 cells transfected with the gene encoding the